Antiviral Research 226 (2024) 105888

Contents lists available at ScienceDirect

Antiviral Research

journal homepage: www.elsevier.com/locate/antiviral

An allosteric inhibitor of sirtuin 2 blocks hepatitis B virus covalently closed circular DNA establishment and its transcriptional activity

Liudi Tang [a,b,*], Stacy Remiszewski [a], Andrew Snedeker [b], Lillian W. Chiang [a], Thomas Shenk [a,c]

[a] Evrys Bio, LLC, Pennsylvania Biotechnology Center, Doylestown, PA, 18902, USA
[b] Baruch S. Blumberg Institute, Doylestown, PA, 18902, USA
[c] Department of Molecular Biology, Princeton University, Princeton, NJ, 08540, USA

ARTICLE INFO

Keywords:
Hepatitis B virus
cccDNA synthesis
Viral transcription
SIRT2
Antiviral

ABSTRACT

296 million people worldwide are predisposed to developing severe end-stage liver diseases due to chronic hepatitis B virus (HBV) infection. HBV forms covalently closed circular DNA (cccDNA) molecules that persist as episomal DNA in the nucleus of infected hepatocytes and drive viral replication. Occasionally, the HBV genome becomes integrated into host chromosomal DNA, a process that is believed to significantly contribute to circulating HBsAg levels and HCC development. Neither cccDNA accumulation nor expression from integrated HBV DNA are directly targeted by current antiviral treatments. In this study, we investigated the antiviral properties of a newly described allosteric modulator, FLS-359, that targets sirtuin 2 (SIRT2), an NAD^+-dependent deacylase. Our results demonstrate that SIRT2 modulation by FLS-359 and by other tool compounds inhibits cccDNA synthesis following *de novo* infection of primary human hepatocytes and HepG2 (C3A)-NTCP cells, and FLS-359 substantially reduces cccDNA recycling in HepAD38 cells. While pre-existing cccDNA is not eradicated by short-term treatment with FLS-359, its transcriptional activity is substantially impaired, likely through inhibition of viral promoter activities. Consistent with the inhibition of viral transcription, HBsAg production by HepG2.2.15 cells, which contain integrated HBV genomes, is also suppressed by FLS-359. Our study provides further insights on SIRT2 regulation of HBV infection and supports the development of potent SIRT2 inhibitors as HBV antivirals.

1. Introduction

Infection by hepatitis B virus (HBV) can lead to chronic disease resulting in progressive liver fibrosis, cirrhosis, and hepatocellular carcinoma. Even though an HBV vaccine was approved by the US FDA in 1981 and global prevalence is slowly declining, 296 million people are still chronically infected, predisposing them to end-stage liver diseases (Hsu et al., 2023). Current methods to treat chronic hepatitis B (CHB) include pegylated interferon (IFN-α) that modulates the immune system and nucleoside or nucleotide analogs (NUCs) that directly target the HBV-coded polymerase to block viral replication. Both treatments slow disease progression and reduce deaths from CHB-associated liver diseases, but rarely lead to a cure which is defined as loss of virus, loss of hepatitis B surface antigen (HBsAg) and HBsAg antibody (HBsAb) seroconversion (Alter et al., 2018; Liang et al., 2015). Thus, most CHB patients must actively manage life-long antiviral treatment, highlighting the urgent need to develop novel therapeutics to cure CHB.

HBV virions deliver a partially double-stranded viral genome, relaxed circular (rc) DNA, to hepatocytes (Huang et al., 2012; Macovei et al., 2010). In the nucleus, cellular DNA repair factors, convert rcDNA into covalently closed circular DNA (cccDNA) (Testoni and Ploss, 2023; Wei and Ploss, 2021) that persists as a low-copy number mini-chromosome, hosting viral transcription (Nassal, 2015). HBV replicates through an RNA intermediate, pregenomic RNA (pgRNA) that is encapsidated in the cytoplasm together with the viral polymerase whose reverse transcriptase activity produces a partially double-stranded DNA genome, rcDNA. Capsids containing rcDNA can be enveloped and exit the cell or they can directly re-enter the nucleus where the viral genome is repaired to replenish cccDNA. NUCs block the reverse transcription of pgRNA, but do not eliminate viral gene expression, due at least in part to the long half-life of cccDNA. The cccDNA pool is reduced but, in most cases, not eliminated during years of NUC treatment (Boyd et al., 2016; Lai et al., 2017); it acts as a reservoir causing relapse of the chronic infection after withdrawal of therapy. In addition, a minor species called double-stranded linear (dsl) DNA derived from the replication of HBV can integrate into the host

* Corresponding author. Evrys Bio, LLC, Pennsylvania Biotechnology Center, Doylestown, PA, 18902, USA.
E-mail address: liudi.tang@bblumberg.org (L. Tang).

https://doi.org/10.1016/j.antiviral.2024.105888
Received 29 November 2023; Received in revised form 10 April 2024; Accepted 12 April 2024
Available online 18 April 2024

genome (Bill and Summers, 2004). It cannot support viral replication, but is capable of producing HBsAg, and thus contributes to viral pathogenesis.

Sirtuins (SIRT1-7) are a family of seven cellular deacylases that use NAD + as a co-factor to catalyze the removal of acyl groups from substrate protein lysine residues, and yield nicotinamide (NAM) and 2′-O-acyl-ADP ribose (Feldman et al., 2012; Hoff et al., 2006). Although de-acetylation is their most extensively studied activity, SIRTs can also remove longer acyl chains, for instance, lysine myristoyl groups (Feldman et al., 2013; Teixeira et al., 2020). Knockdown of SIRTs alters the growth of multiple DNA and RNA viruses (Hackett et al., 2019; Koyuncu et al., 2014; Roche et al., 2023). In the case of HBV, genetic manipulation of SIRTs suggested that SIRT1 (Ren et al., 2014), SIRT2 (Piracha et al., 2018; Qu et al., 2022; Wu et al., 2022), and SIRT6 (Jiang et al., 2019) are proviral, whereas SIRT3 (Ren et al., 2018) and SIRT7 (Yu et al., 2021) are antiviral factors. In line with genetic evidence, a SIRT2-modulating tool compound, AGK2, exhibits anti-HBV activity in cultured cells and in HBV transgenic mice (Piracha et al., 2018; Yu et al., 2018). These data provide strong support for the view that SIRT2 is a potential therapeutic target for HBV infection (Poniewierska-Baran et al., 2022).

Our group recently reported a new class of allosteric SIRT2 modulators, exemplified by FLS-359, that exhibit antiviral activity against multiple DNA and RNA viruses (Roche et al., 2023). In this present work, we explored the antiviral activity of FLS-359 against HBV and found that the compound blocks cccDNA establishment when present from the beginning of the infection. When dosed after cccDNA establishment, FLS-359 reduces viral RNA production, likely due to suppression of HBV promoter activities, and it decreases the extracellular accumulation of HBsAg from cells with integrated HBV. Our study sheds new light on the mechanisms by which SIRT2 regulates the HBV replication cycle and lends further support to the development of SIRT2 modulators as HBV antivirals.

2. Materials and methods

2.1. Cells, viruses, chemicals, antibodies

HepG2 cells were from ATCC (ATCC HB-8065). C3A-NTCP cells (Guo et al., 2017) were provided by Dr. Ju-Tao Guo (Baruch S. Blumberg Institute). The HepG2.2.15 cell line was licensed from Millipore (Millipore-Sigma SCC249). Cells were cultured in high glucose DMEM medium (Cleveland Clinic Media Core) with 10% FBS, 100 U/ml penicillin, and 100 μg/ml streptomycin. The HepAD38 cell line (Ladner et al., 1997) was a gift from Dr. Christoph Seeger (Fox Chase Cancer Center), and was cultured in DMEM/F12 medium (Corning) with 10% FBS, 100 U/ml penicillin, 100 μg/ml streptomycin, and 1 μg/ml tetracycline. Primary human hepatocytes (PXB cells), passaged in immunodeficient mice, were purchased from PhoenixBio and cultured in dHCGM medium (PhoenixBio). All cells were maintained in a 5% CO_2 incubator at 37 °C. HepAD38 cell-derived genotype D HBV used for infecting hepatocytes were purchased from ImquestBio. Recombinant adenovirus expressing inducible HBV 2.1 kb RNA (Ad-HBV2.1) was provided by Dr. Tianlun Zhou (Baruch S. Blumberg Institute). FLS-359 was synthesized as described in US Patent Application US20210139475A1. NMR analysis was consistent with the structure, and purity was determined to be greater than 97% by reversed-phase HPLC. The following reagents were purchased: Myrcludex B (MyrB, Aobious); Entecavir, AGK2, SirReal2, and Cambinol (Sigma-Aldrich); TM (Abmole Bioscience); RG7834 (MedChemExpress); human recombinant interferon-α/2 b (BPS Bioscience); HBc antibody for HBV particle gel assay (C1-5, sc-23945, Santa Cruz Biotechnology); HBc antibody for Western blot (T2221, catalog no. 2AHC24, Tokyo Future Style); SIRT2 antibody (ab211033, Abcam); α-tubulin antibody (catalog no. 3873, Cell Signaling Technology); and β-actin antibody (MA1-140, Invitrogen).

2.2. Plasmids

HBV promoter/enhancer regions including PreS1p (2219–2780), PreS2p (2809–3152), EnhI/Xp (1060–1375), and EnhII/Cp (1643–1849) were PCR amplified from cccDNA extracted from HBV-infected C3A-NTCP cells, and inserted into the pGL3-basic luciferase reporter vector (Promega Biosciences). The plasmids are sequence confirmed and designated as pGL3-PreS1p, pGL3-PreS2p, pGL3-EnhI/Xp, and pGL3-EnhII/Cp. Primer sequences used to clone the HBV promoter/enhancer regions into pGL3-basic vector are listed in Table S1. The reporter plasmid for activity of the HCMV immediate-early promoter, pGL3-CMV-IEp, was obtained from Dr. Eain Murphy (Upstate Medical University). The plasmids replicating HBV genotypes A-D were previously described (Wu et al., 2018).

2.3. Establishment of the C3A-NTCP-SIRT2 cell line

The cDNA clone encoding FLAG-tagged full-length SIRT2 isoform 1 was purchased from Genscript (Clone ID OHu17572). The coding sequence of SIRT2 was cloned with primers 5′-CCGGAATTCATGGCAGAGCCAG-3′ and 5′- ATAGTTTAGCGGCCGCTCACTGGGGTTTC-3’. The resulting PCR product was digested with *Eco*RI and *Not*I before inserting into pCX4bsr retroviral vector (NovoPro Bioscience Inc) that underwent the same restriction digestion. Pseudotyped retroviruses were packaged in GP2-293 with the helper plasmid pVSV-G, and then used to transduce C3A-NTCP cells. After selecting with medium containing 10 μg/ml of Blasticidin, drug-resistant cells were expanded and designated as C3A-NTCP-SIRT2, with the expression of SIRT2 confirmed by Western blot assay.

2.4. HBV infection of hepatocytes

PXB-cells were infected with HBV genotype D at 500 genome equivalents/cell (GEs/cell) in dHCGM medium supplemented with PEG-8000 (Sigma P1458) to a final concentration of 4%. The inoculum was removed at 24 hpi and the cell monolayers were washed with PBS three times before feeding with dHCGM medium. For infection assay using C3A-NTCP cells, conditioned medium (DMEM supplemented with 3% FBS, 2% DMSO, 1 × non-essential amino acids) was applied to newly seeded C3A-NTCP cells for one day prior to HBV infection. After infection with HBV at the indicated GEs/cell in conditioned medium supplemented with 4% PEG-8000 for 24 h, the inoculum was removed and monolayers were washed with PBS three times, and then maintained in conditioned medium.

2.5. Assays for HBV DNA, RNA and proteins

For analysis of viral DNAs, extraction of cytoplasmic HBV core DNA and Hirt DNA were performed as described (Tang et al., 2019). For Southern blots, extracted DNA samples were resolved by electrophoresis in 1.2% agarose gels; transferred to an Hybond-XL membrane (GE Healthcare); crosslinked using a UV crosslinker; hybridized with a^{32}P-labeled full-length plus strand HBV riboprobe, or with a DIG-labeled full length HBV DNA probe; and the resulting bands were detected using a Typhoon scanner or a BioRad ChemiDoc imaging system, respectively. To facilitate the detection of HBV cccDNA by Southern blot, Hirt DNA samples were heated at 88 °C for 8 min to denature the protein-free rcDNA/DP-rcDNA into single-stranded DNA, followed by digestion with *Eco*RI to linearize supercoiled cccDNA into unit-length double-stranded linear DNA (denoted as cccDNA/*Eco*RI). Quantification of HBV cccDNA by real-time PCR (Xia et al., 2017), used primers 971-GCCTATTGATTGGAAAGTATGT-992 (sense) and 1994-AGCTGAGGCGGTATCTA-2010 (antisense) with the LightCycler 480 SYBR green I Master PCR kit (Roche) under the following PCR program: denaturation at 95 °C for 10 min, followed by 45 cycles of amplification consisting of 95 °C for 15 s, 60 °C for 5 s, 72 °C for 45 s, and 88 °C for 2 s.

For analysis of viral RNA, total RNA was extracted using TRIzol

reagent (Invitrogen). For Northern blots, RNA samples were resolved by electrophoresis in 1.2% agarose gels; transferred to an Hybond-XL membrane (GE Healthcare); crosslinked using a UV crosslinker; hybridized with a ^{32}P-labeled full-length minus strand HBV riboprobe, or with a DIG-labeled full length HBV DNA probe; and the resulting bands were detected using a Typhoon scanner or a BioRad ChemiDoc imaging system, respectively. Detection of HBV RNA using real-time RT-PCR was conducted by using SuperScript III Platinum One-Step qRT-PCR kit (Invitrogen). Primers 1521-ACGGGGCGCACCTCTCTTTA-1540 (sense) and 1577- GTGAAGCGAAGTGCACACGG-1596 (antisense) that target the overlapping region of all HBV RNA transcripts were used to quantify the abundance of total HBV RNA. As an internal control, primers CACCATTGGCAATGAGCGGTTC (sense) and AGGTCTTTGCGGATGTCCACGT (antisense) that target the cellular β-actin gene were used. The real-time RT-PCR program was carried out following the manufacturer's protocol.

HBeAg and HBsAg secreted into culture supernatant were detected by using HBeAg and HBsAg CLIA assay kits (Ig Biotechnology) following the manufacturer's protocol. Drug treated cultures were fixed with 2% paraformaldehyde, stained with 4′,6-diamidino-2-phenylindole (DAPI), imaged by BioTek Cytation 3 to determine nuclei counts as an indicator of cell viability.

2.6. HBV particle gel assay

Cells grown in a 12-well plate were lysed in 400 μL lysis buffer containing 10 mM Tris-HCl pH 8.0, 1 mM EDTA, 1% NP40. After centrifugation (12,000×*g*, 10 min, 4 °C), nuclei were removed, and 20 μL cytoplasmic lysates that contain HBV capsids were resolved in a native 1.0% agarose gel by electrophoresis and transferred onto an Hybond-XL membrane (GE Healthcare). After fixing the membrane with 2.5% paraformaldehyde and 50% methanol, the membrane was blotted with anti-HBc antibody (C1-5, Santa Cruz sc-23945) at 4 °C overnight. Bound antibodies were revealed by IRDye 680RD anti-mouse secondary antibodies (LiCor) and visualized with the Li-COR Odyssey CLX system.

2.7. Western blot assay

Cells grown in 6-well plate were lysed in 1 × NuPAGE LDS sample buffer (250 μL) (Thermo Fisher) supplemented with 2.5% 2-mercaptoethanol. After boiling for 10 min, lysates were loaded on a SurePAGE Bis-Tris 4–20% gel (Genscript), and resolved in MOPS-SDS buffer. An iBlot 2 blotting system was used to transfer proteins from the gel onto a polyvinylidene difluoride (PVDF) membrane. The membrane was reacted with indicated primary antibodies at 4 °C overnight. Bound antibodies were revealed by IRDye 680RD anti-mouse or IRDye 800 C W anti-Rabbit secondary antibodies (LiCor) and visualized with the Li-COR Odyssey CLX system.

2.8. Luciferase reporter assay

HepG2 cells were transfected with HBV promoter reporter plasmids pGL3-PreS1p, pGL3-PreS2p, pGL3-EnhI/Xp, and pGL3-EnhII/Cp, and control plasmid pGL3-CMV-IEp. 24 h after transfection, medium was refreshed, and cells were treated with FLS-359 at various concentrations for another 24 h before analyzing the luciferase activity using the firefly luciferase assay system (Promega) with the BioTek Cytation 3 plate reader.

2.9. Statistics

Quantitative results are presented as mean ± SD of independent experiments. Statistical significance was determined using GraphPad Prism 8 b y conducting the unpaired student t-tests between two groups, or one-way ANOVA with Dunnett's multiple comparison correction (for multiple comparisons). Significance was set at a P value < 0.05.

3. Results

3.1. FLS-359 inhibits cccDNA establishment following de novo HBV infection

Multiple RNA and DNA viruses were found to be inhibited by FLS-359 with IC_{50}s ranging from 0.3 to 6.7 μM (Roche et al., 2023), so we initially used primary human hepatocytes (PXB-cells) to test the utility of FLS-359 as an HBV antagonist at 2.5, 5.0 and 10 μM. Drug was added 4 h before infection and maintained in the medium until harvesting 6 dpi (Fig. 1A). It reduced the amount of HBV cccDNA at each of the three doses (Fig. 1B). Total HBV RNA was more substantially reduced than cccDNA when infected cells were treated with FLS-359 at 5 μM and 10 μM (Fig. 1C). Moreover, the reduction in total HBV RNA correlated with the loss of HBsAg and HBeAg in the culture supernatant (Fig. 1D–E). The HBV entry inhibitor Myrcludex B (MyrB) was included as a positive control, and it abolished cccDNA establishment, blocking the subsequent accumulation of viral replication products. To rule out the possibility that the FLS-359 antiviral activity simply resulted from cell toxicity, uninfected PXB-cells were treated with drug (1.25–20 μM) for 8 days and assayed for viability (Fig. 1F). No toxicity was evident.

We confirmed FLS-359 anti-HBV activity in C3A-NTCP cells that express the cell receptor for the virus. It has been reported that SIRT2 modulation is anti-proliferative or cytotoxic for certain tumor cell lines (Jing et al., 2016; Wang et al., 2019). Thus, C3A-NTCP cells were exposed to FLS-359 only during the first 2 days of HBV infection, which avoided compromising cell viability (Fig. S2B), and viral assays were performed at 6 dpi (Fig. 2A). Southern blot analysis showed that HBV cccDNA was reduced after FLS-359 treatment (Fig. 2B), as were HBV 3.5 kb RNA and HBs RNAs (Fig. 2C), HBV cytoplasmic core DNA (Fig. 2D), HBc (Fig. 2E), and secreted HBeAg and HBsAg (Fig. 2F–G). As expected, MyrB completely blocked the accumulation of cccDNA and its products; ETV did not significantly alter *de novo* cccDNA synthesis because the viral polymerase is not essential for rcDNA to cccDNA conversion (Wei and Ploss, 2021), yet it substantially reduced the replication-dependent cytoplasmic core DNA (Fig. 2D). In agreement with its known inhibition of cccDNA transcription (Cheng et al., 2020; Shen et al., 2018; Tropberger et al., 2015), IFN-α reduced HBV 3.5 kb RNA, HBc and HBeAg production without significantly reducing cccDNA levels (Fig. 2). Of note, we did not observe reductions in HBV 2.4/2.1 HBs RNA and HBsAg levels (Fig. 2). The experiment was repeated in C3A-NTCP cells assaying cccDNA at 2 dpi by qPCR assay (Fig. S1). Using this quantitative assay, the IC_{50} for cccDNA inhibition by FLS-359 was <0.625 μM, and the maximum inhibition achieved was 94.3% at 10 μM drug. Taken together, these data suggest that FLS-359 impairs HBV infection of PXB and C3A-NTCP cells, at least in part by curtailing the establishment of cccDNA.

To examine whether inhibition of HBV infection is a shared feature of SIRT2 inhibitors, we tested several chemically distinct tool compounds targeting SIRT2 or SIRT1/2, namely AGK2 (Wang et al., 2019), TM (Jing et al., 2016), and Cambinol (Heltweg et al., 2006). Treatment with these compounds during the first 2 days of HBV infection in C3A-NTCP cells all resulted in a dose-dependent reduction of HBeAg at 6 dpi (Fig. S2A). AGK2 has been shown to inhibit HBV replication previously (Piracha et al., 2018; Yu et al., 2018). Compounds were well-tolerated by C3A-NTCP cells, except for the highest concentration of TM tested (100 μM) (Fig. S2B). Similar to FLS-359, AGK2 and TM treatment reduced cccDNA accumulation following *de novo* HBV infection of C3A-NTCP cells (Fig. S2C). In addition, while ectopic expression of SIRT2 slightly elevated the HBeAg production following HBV infection, treatment with FLS-359, AGK2 and TM all reversed the promoting effect of SIRT2 (Fig. S3). Since these compounds have distinct chemical scaffolds, our result argues that FLS-359 inhibits HBV infection through SIRT2 modulation.

To evaluate whether FLS-359 affects HBV early entry steps, we modified a synchronized HBV internalization assay protocol

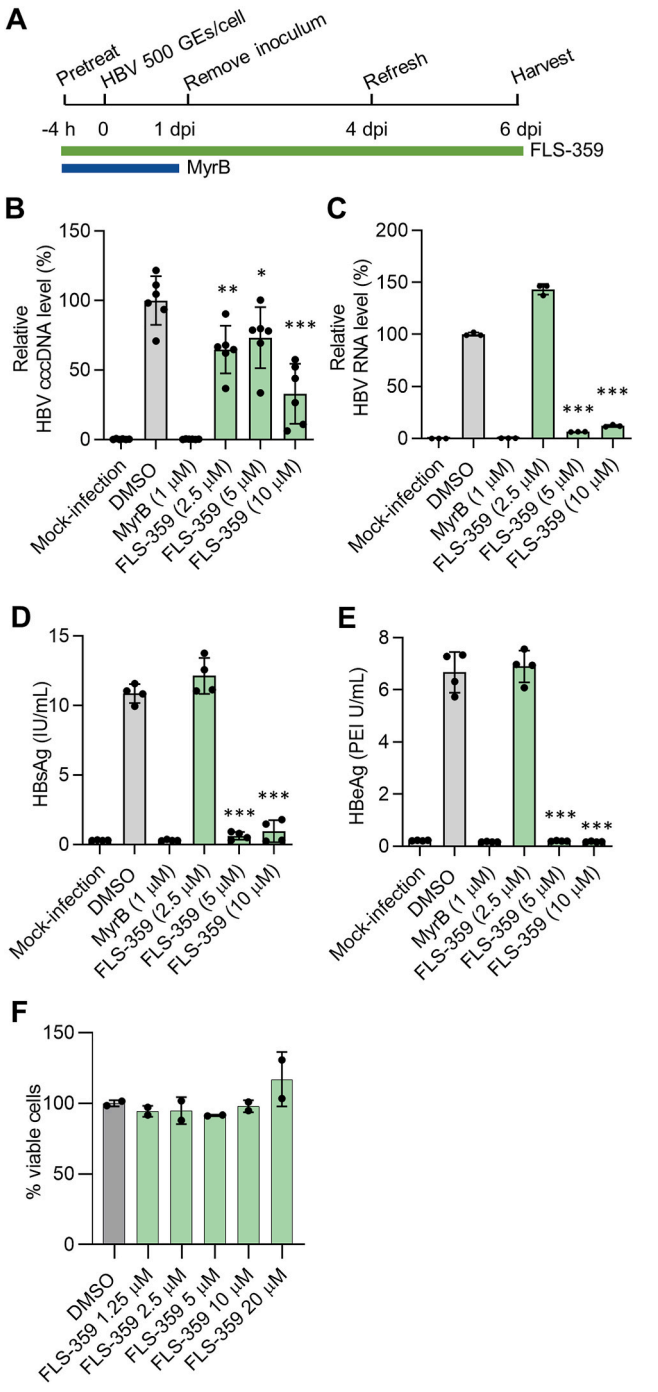

Fig. 1. FLS-359 blocks HBV infection in primary human hepatocytes. (**A**) Schematic representation of the virus infection and compound treatment schedule. PXB-cells were mock-infected or infected with HBV (500 GE s/cell), treated with DMSO or FLS-359 in DMSO from 4 h prior to the infection to 6 dpi, or with MyrB 4 h prior to the infection to 1 dpi. Cells and culture supernatant were harvested at 6 dpi. (**B**) HBV cccDNA was quantified by qPCR and normalized to the infected- and DMSO-treated group. Mean ± SD is shown (n = 3, each with 2 qPCR technical repeats). (**C**) Total HBV RNA transcripts were quantified by RT-qPCR and normalized to cellular β-actin RNA. Data are presented as HBV RNA levels relative to the infected- and DMSO-treated group. Mean ± SD is shown (n = 3). HBsAg (**D**) and HBeAg (**E**) secreted into culture supernatant from 4 to 6 dpi were quantified by CLIA assay. Mean ± SD is shown (n = 4). (**F**) PXB cells were treated with DMSO or FLS-359 in DMSO at indicated concentrations for 8 days; cells were washed with PBS and fixed with 2% paraformaldehyde, followed by DAPI staining. Cell viability was determined by DAPI cell count, and normalized to the DMSO-treated group. Mean ± SD is shown (n = 2). *$p < 0.05$; **$p < 0.01$; ***$p < 0.001$.

(Chakraborty et al., 2020) and tested if FLS-359 blocks the uptake of HBV DNA. Our result indicates that a 6 h FLS-359 treatment during HBV internalization did not significantly reduce the amount of intracellular HBV DNA, as opposed to the entry inhibitor MyrB (Fig. S4). The cellular housekeeping gene GAPDH served as a control. In addition to cccDNA synthesis during *de novo* infection, rcDNA in progeny nucleocapsids can shuttle back to the nuclei of infected cells to replenish the cccDNA pool, via the intracellular cccDNA amplification (recycling) pathway (Tuttleman et al., 1986). To test whether FLS-359 blocks intracellular cccDNA amplification, a rapid and synchronized cccDNA formation assay in HepAD38 cells was employed (Sheraz et al., 2019). Tetracycline (tet) removal from HepAD38 cells initiates HBV replication, which is arrested at the single-stranded (ssDNA) stage by a reversible polymerase inhibitor phosphonoformic acid (PFA). Intracellular cccDNA amplification from the accumulated ssDNA precursor takes place rapidly after PFA removal. While a 36 h treatment with FLS-359 (5 μM or 10 μM) slightly increased the amount of cytoplasmic HBV core DNA, its conversion to cccDNA was substantially blocked (Fig. S5). AGK2 showed a trend toward reduced cccDNA production, but did not reach significance. These experiments together argue that FLS-359 acts after cell entry to block conversion of rcDNA to cccDNA, at a step that blocks cccDNA production from both *de novo* infection and intracellular recycling.

3.2. Short-term treatment with FLS-359 does not degrade existing cccDNA but reduces viral RNA accumulation

HBV cccDNA is the most refractory replication intermediate to the current anti-HBV regimen, and the inability to eliminate cccDNA is one of the major reasons for persistent infection and viral rebound after treatment cessation (Guo and Guo, 2015). Since cccDNA was markedly reduced when hepatocytes were exposed to FLS-359 from the beginning of HBV infection (Figs. 1–2, and S1), we next tested whether FLS-359 triggers the decay of pre-existing cccDNA molecules. To this end, we infected PXB-cells with HBV for 4 days to allow cccDNA establishment (Lee et al., 2021; Qi et al., 2016), followed by FLS-359 treatment for another 6 days (Fig. 3A). ETV (1 μM) was added to block potential cccDNA replenishment from its recycling pathway. Delayed treatment with FLS-359 did not change the amount of cccDNA (Fig. 3B). Notwithstanding, total HBV RNA, secreted HBsAg and HBeAg were all markedly reduced in the 10 μM FLS-359-treated group (Fig. 3C–E).

To further probe the impact of FLS-359 treatment on pre-existing cccDNA levels and transcriptional activity, C3A-NTCP cells were infected with HBV for 4 days before drug treatment from 4 dpi to 6 dpi (Fig. 4A). Consistent with PXB cells, cccDNA amounts were not altered by FLS-359 (Fig. 4B and Fig. S6). Nevertheless, HBV RNA species were markedly reduced (Fig. 4C), as were cytoplasmic core DNA, HBc, and secreted HBeAg and HBsAg in the culture supernatant (Fig. 4D–G). Notably, while all SIRT2 tool compounds reduced HBeAg levels in a dose-dependent manner when blocking HBV *de novo* infection (Fig. S2), the drugs were less effective in reducing HBeAg production from established cccDNA in C3A-NTCP cells (Fig. S7). In fact, AGK2 had very little effect on HBeAg production under these conditions. This discrepancy could be due to subtly different modes of action of the SIRT2 modulators, perhaps differentially affecting distinct SIRT2 functions, e.g., removal of different types of acyl groups (Roche et al., 2023), involved in the HBV life cycle.

3.3. FLS-359 reduces HBV RNA and antigen production in HepG2.2.15 cells

Although HBV integrated into the host chromosome cannot support productive viral replication, it can nevertheless direct HBsAg production and contribute to HBV immune-tolerance and pathogenesis (Ghany and Lok, 2022; Tu et al., 2017). Accordingly, we employed HepG2.2.15 cells to model the possible effect of FLS-359 on gene expression from

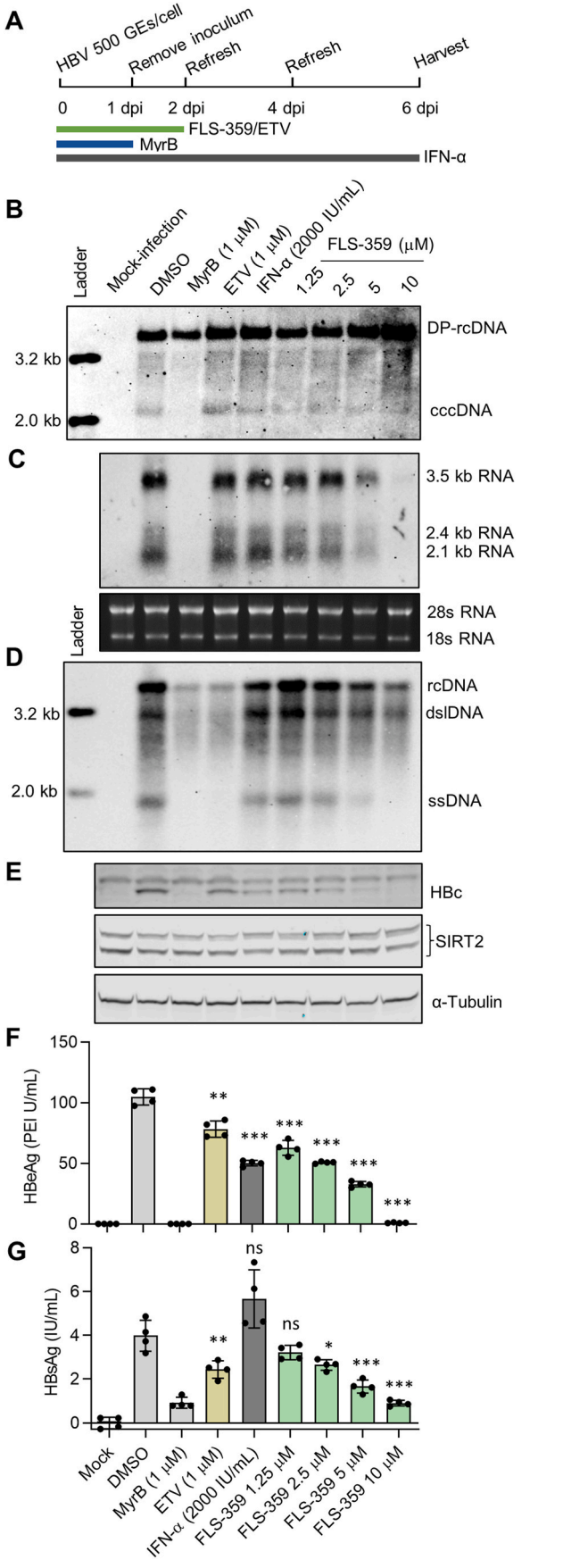

Fig. 2. FLS-359 reduces HBV cccDNA establishment in C3A-NTCP cells. (**A**) Schematic representation of the virus infection and compound treatment schedule. C3A-NTCP cells were mock-infected or infected with HBV (2000 GE s/cell), and treated with DMSO or with drugs in DMSO at indicated concentrations and time frames. Cells and culture supernatant were harvested at 6 dpi. (**B**) Hirt DNA was extracted and analyzed by Southern blot assay using DIG-labeled full length HBV DNA probe. The cccDNA and DP-rcDNA are labeled. (**C**) Total RNA was resolved by Northern blot assay using DIG-labeled full length HBV DNA probe. HBV 3.5 kb RNA, 2.4 kb RNA, and 2.1 kb RNA are labeled. 18 S and 28 S ribosomal RNA serve as internal controls. (**D**) Replicative cytoplasmic core DNA was resolved by Southern blot assay using DIG-labeled full length HBV DNA probe. rcDNA, dslDNA, and ssDNA are labeled. (**E**) The levels of HBV core protein (HBc), SIRT2, and α-tubulin were determined by Western blot assay. (**F-G**) HBeAg and HBsAg secreted into culture medium from 4 to 6 dpi were quantified by CLIA assay. Mean ± SD is shown (n = 4). *$p < 0.05$, **$p < 0.01$, ***$p < 0.001$.

integrated HBV DNA (Fig. 5A). In addition to HBV cccDNA, HepG2.2.15 cells contain two unit-length HBV genome copies integrated into the host chromosome that include their authentic promoters (Sureau et al., 1986). Treatment with FLS-359 for 2 days had no measurable effect on cell viability (Fig. S8B), but it reduced HBV 3.5 kb and 2.4/2.1 kb RNAs in a dose dependent manner (Fig. 5B). The reduction in HBV RNA species correlates with a decline in cytoplasmic HBV ssDNA, HBV capsid particles and secreted HBeAg and HBsAg in the culture supernatant (Fig. 5C–F). ETV was used as a control to indicate the baseline cytoplasmic HBV core DNA level since HBV replicates constitutively in HepG2.2.15 cells (Fig. 5C). As expected, ETV treatment did not alter the levels of HBV capsids and secreted HBsAg, but slightly increased HBV RNA amount. Interestingly, the reduction of ssDNA did not lead to a proportional decrease of rcDNA when cells were treated with higher concentrations of FLS-359 (Fig. 5C). Considering that 2.4 kb/2.1 kb HBs RNA and secreted HBsAg are dramatically reduced by FLS-359, we speculate that disruption of the HBV envelope component might lead to intracellular retention of rcDNA-containing envelopment-competent nucleocapsids but not ssDNA-containing envelopment-incompetent particles (Hu and Liu, 2017).

Next, we compared the activity of FLS-359 with other SIRT2 tool compounds in reducing HBsAg production from HepG2.2.15 cells (Fig. S8). The experiment was performed as in Fig. 5A. FLS-359 and TM showed dose-dependent activity, but, as seen for HBV-infected C3A-NTCP cells (Fig. S7), AGK2 showed limited activity, while Cambinol and SirReal2 (Rumpf et al., 2015), only slightly reduced HBsAg at relatively high concentrations. RG-7834, which targets host PAPD5/7 poly(A) polymerases essential for HBV RNA stability (Han et al., 2018; Mueller et al., 2019), was included as a positive control. As before, the fact that multiple SIRT2 modulators reduce HBsAg production argues that SIRT2 is a critical target in HepG2.2.15 cells.

3.4. Reduction of HBV RNA and protein accumulation occurs rapidly after FLS-359 treatment

We next focused on how quickly FLS-359 exhibits its antiviral effects. Infected C3A-NTCP cells were treated with DMSO or FLS-359 (10 μM) in DMSO for 3, 6, 12, 24, or 48 h beginning at 5 dpi before harvesting (Fig. 6A). Strikingly, the extracellular accumulation of HBeAg was blocked throughout the time period and became statistically significant due to an HBeAg increase in the absence of drug after 12 h of FLS-359 treatment (Fig. 6B). An increasing reduction in total HBV RNA was also detected when comparing FLS-359-treated cultures to the DMSO control (Fig. 6C–D). The accumulation of HBsAg in the culture supernatant of HepG2.2.15 cells exposed to FLS-359 was also completely suppressed by FLS-359, becoming notably less than the DMSO control after 6 h of treatment (Fig. 6E–F), correlating with the reduction in total HBV RNA (Fig. 6G–H). These data suggest that FLS-359 acts quickly to reduce the HBV RNA production, which at least in part contributes to the

(caption on next column)

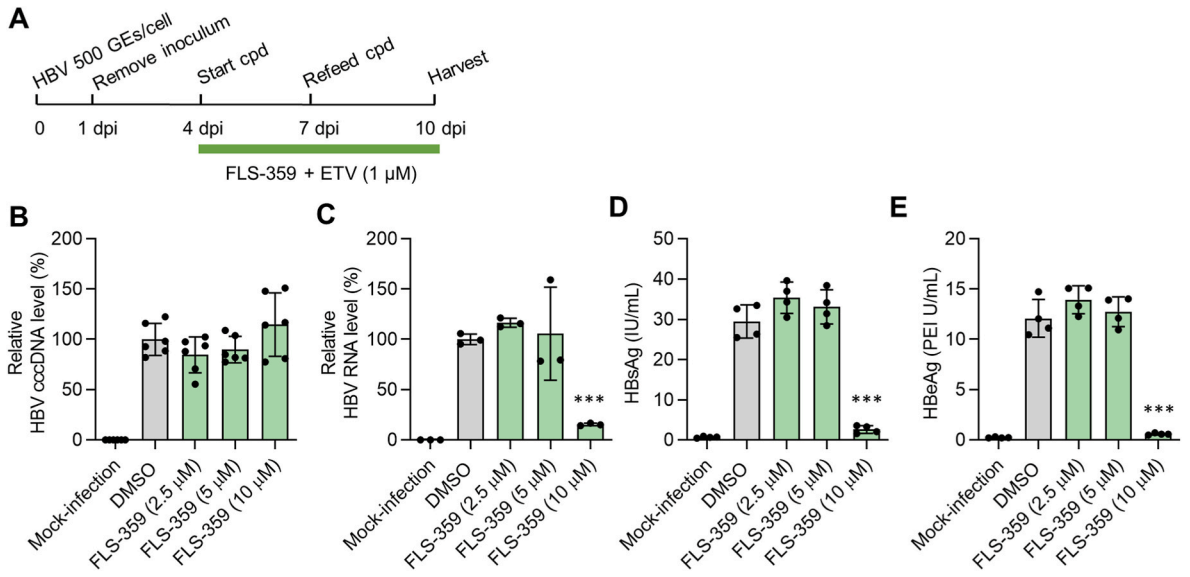

Fig. 3. FLS-359 reduces HBV RNA production in HBV-infected primary human hepatocytes. (**A**) Schematic representation of the virus infection and compound treatment schedule. PXB cells were mock-infected or infected with HBV (500 GE s/cell). From 4 dpi, 1 μM ETV was maintained in cultures to block the potential replenishment of cccDNA through the recycling pathway, and cells were treated with DMSO or FLS-359 in DMSO at indicated concentrations until harvesting cells and culture supernatants at 10 dpi. (**B**) Hirt DNA was extracted, and HBV cccDNA was quantified by qPCR and normalized to the DMSO-treated group. Mean ± SD is shown (n = 3, each with 2 qPCR technical repeats). (**C**) Total RNA was extracted from cells, and HBV RNA was quantified by RT-qPCR and normalized to cellular β-actin RNA amounts. Data are presented as HBV RNA levels relative to the DMSO-treated group. Mean ± SD is shown (n = 3). HBsAg (**D**) and HBeAg (**E**) secreted into culture medium from 7 to 10 dpi were quantified by CLIA assay. Mean ± SD is shown (n = 4). ***p < 0.001.

reduced antigen levels in the culture supernatants. The extent of the viral antigen reduction in the culture supernatant is much more profound than the intracellular HBV RNA reduction, arguing that the drug also exerts post-transcriptional effects on the production of extracellular viral antigens.

3.5. FLS-359 impairs HBV promoter activities

Reduced HBV RNA accumulation in FLS-359-treated hepatocytes could result from less viral RNA production or by accelerated decay. To test whether FLS-359 promotes HBV RNA decay, recombinant adenovirus expressing HBV 2.1 kb RNA in a doxycycline-(off) dependent manner (Ad-HBV2.1) was employed (Sun et al., 2020). HepG2 Cells were infected with Ad-HBV2.1 for 3 days to induce accumulation of HBsAg-expressing 2.1 kb RNA (Fig. 7A), after which doxycycline was added to stop viral RNA synthesis. Then viral RNA levels were monitored after various time intervals in the presence of DMSO, FLS-359 or RG-7834 (Fig. 7B). Unlike treatment with RG-7834, a dihydroquinolizinone known to destabilize HBV RNAs (Han et al., 2018; Mueller et al., 2018), FLS-359 did not significantly change the abundance of HBV 2.1 kb RNA, indicating that reduced viral RNA accumulation is likely due to FLS-359 inhibition of viral RNA production (Fig. 7C). In support of this argument, promoter-reporter plasmids bearing each of the four HBV promoters/enhancers in HepG2 cells exhibited dose-dependent inhibition in response to FLS-359 treatment (Fig. 7D). In contrast, activity of the human cytomegalovirus promoter was inhibited to a much more limited extent, as described previously (Roche et al., 2023). Thus, FLS-359 works at least in part through suppressing HBV promoter activities to reduce viral RNA levels, consistent with the work of others, who used genetic approaches to demonstrate SIRT2 positive regulation of HBV promoters (Piracha et al., 2018; Wu et al., 2022).

Finally, to evaluate whether FLS-359 is effective against different HBV genotypes, replication competent HBV plasmids derived from genotype A, B, C, and D were transiently transfected into HepG2 cells, and the levels of HBsAg and HBeAg accumulation in the culture supernatant was tested against a range of FLS-359 concentrations (Fig. S9). Although different HBV genotypes yielded varying levels of HBsAg and HBeAg, they all showed similar FLS-359 IC_{50}s. Thus, FLS-359 inhibits gene expression of multiple HBV genotypes.

4. Discussion

Long-term NUC therapy of CHB can efficiently suppress viral replication, but HBsAg loss is rare (Jeng and Lok, 2021). HBV cccDNA is the persistent reservoir for chronic infection and thus the failure to eliminate pre-existing cccDNA molecules and/or prevent new cccDNA establishment by current antiviral regimens can explain the low cure rate of CHB. Elimination of cccDNA is a leading strategy for achieving a cure (Jin et al., 2023; Martinez et al., 2021; Wei and Ploss, 2021; Xia and Guo, 2020; Zoulim and Testoni, 2023). Multiple approaches have been investigated to target cccDNA, including cytokine treatments (Lucifora et al., 2014; Stadler et al., 2021; Xia et al., 2016), activation of innate viral sensors (Lee et al., 2021), gene therapies that include RNAi and CRISPR-Cas9 (Bloom et al., 2018), and small molecule screening campaigns (Jin et al., 2023; Sheraz et al., 2019; Wang et al., 2023), but questions about potency, selectivity and toxicity remain.

Knock-down and overexpression experiments, as well as studies with small molecule SIRT2 modulators, have convincingly shown that SIRT2 supports HBV replication (Cheng et al., 2018; Piracha et al., 2018; Wu et al., 2022; Yu et al., 2018). However, genetic manipulations designed to explore a possible role for SIRT2 in cccDNA production or stability have produced seemingly conflicting results. Piracha and colleagues (Piracha et al., 2020) reported that overexpression of different SIRT2 isoforms either increased or decreased cccDNA levels by several fold, whereas Wu et al. found no effect of SIRT2 overexpression or knockdown (Wu et al., 2022). Here we report that FLS-359 can prevent *de novo* synthesis and intracellular amplification of cccDNA. The small molecule SIRT2 modulator likely impacts cccDNA differently than SIRT2 overexpression or knockdown because the drug exhibits substrate-selective activity (Roche et al., 2023). It inhibits SIRT2-mediated deacetylation but not a different SIRT2 activity, demyristoylation, an enzymatic selectivity reported for other SIRT2 modulators as well (Lin, 2023). As a result, the activity of the small molecules is distinct from effects of

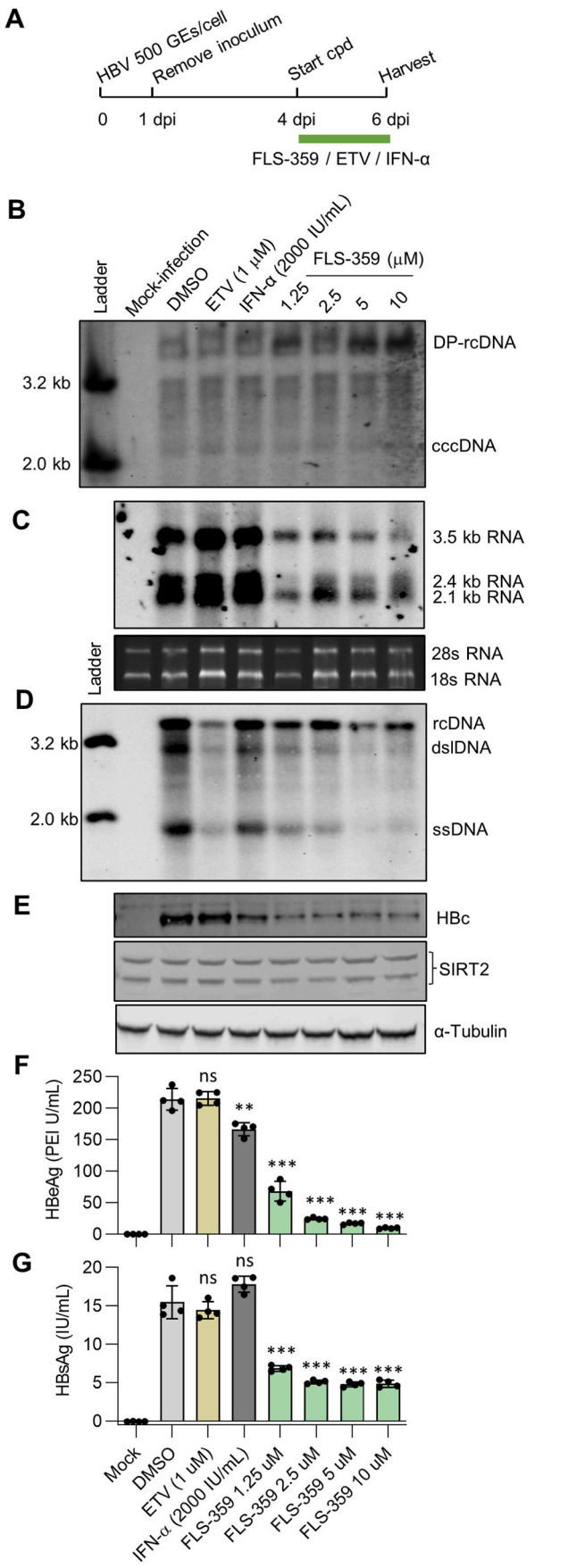

(caption on next column)

Fig. 4. FLS-359 does not induce degradation of existing cccDNA, but reduces HBV RNA accumulation in C3A-NTCP cells. (A) Schematic representation of the virus infection and compound treatment schedule. C3A-NTCP cells were mock-infected or infected with HBV (2000 GE s/cell). From 4 to 6 dpi, cells were treated with DMSO or drugs in DMSO at indicated concentrations. Cells and culture supernatant were harvested at 6 dpi. (**B**) Hirt DNA was extracted and resolved by Southern blot assay using DIG-labeled full length HBV DNA probe. cccDNA and DP-rcDNA are labeled. (**C**) Total RNA was extracted from cells and analyzed by Northern blot assay using DIG-labeled full length HBV DNA probe. HBV 3.5 kb RNA, 2.4 kb RNA, and 2.1 kb RNA are labeled. 18 S and 28 S ribosomal RNA serve as internal controls. (**D**) Replicative cytoplasmic coreDNA was extracted and analyzed by Southern blot assay using DIG-labeled full length HBV DNA probe. rcDNA, dslDNA, and ssDNA were denoted. (**E**) The levels of HBV core protein (HBc), SIRT2, and α-tubulin were determined by Western blot assay. (**F-G**) Secreted HBeAg and HBsAg that accumulated from 4 to 6 dpi were quantified by CLIA assay. Mean ± SD is shown (n = 4). $^{**}p < 0.01$, $^{***}p < 0.001$.

genetic manipulations.

Short-term FLS-359 treatment at the time of infection markedly blocked cccDNA establishment (Figs. 1 and 2, S1, and S2), although the drug was not able to eliminate pre-existing cccDNA within the relatively short timeframes tested (Figs. 3 and 4). The fact that additional SIRT2 inhibitors, such as AGK2 and TM, can reduce establishment of cccDNA following *de novo* infection (Fig. S2C) lends strong support to the view that FLS-359 acts through SIRT2 to target cccDNA. Although the molecular mechanism warrants further investigation, our results point to a possible de-acylation event essential for cccDNA establishment that is counteracted by SIRT2 modulation. Multiple cellular processes are regulated by protein lysine acylation, including protein-membrane interactions (Okada et al., 2021) and DNA repair (Chen et al., 2022). It is therefore possible that FLS-359 inhibits cccDNA by blocking HBV vesicle trafficking or one or more DNA repair proteins involved in rcDNA to cccDNA conversion.

Is there potential therapeutic benefit of blocking cccDNA establishment upon re-infection or intracellular recycling for CHB? A study using drug-resistance mutations as a biomarker to monitor the intrahepatic cccDNA turnover rate in CHB patients, suggested that the half-life of cccDNA is shorter than previously thought (Huang et al., 2021). This means that a persistent cccDNA pool likely requires constant cccDNA replenishment, so that blocking new cccDNA establishment by modulating SIRT2 has potential to reduce intrahepatic cccDNA levels over time in CHB patients. Furthermore, two recent studies demonstrated that transcriptionally silenced cccDNA can be reactivated upon re-infection with HBV (Allweiss et al., 2022; Peng et al., 2023). The re-introduction of HBx to overcome the SMC5/6 control of previously restricted cccDNA is likely the molecular mechanism. Therefore, similar to an HBV entry inhibitor (Allweiss et al., 2022), it is conceivable that by blocking cccDNA establishment, FLS-359 could inhibit the re-awakening of cccDNA from its silent state imposed by immunosurveillance or by other therapeutic agents.

Despite the fact that FLS-359 cannot purge established cccDNA in the relatively short timeframes we have tested in cultured cells, it significantly decreased cccDNA-driven viral RNA production and subsequent viral replication (Figs. 3 and 4). All four HBV promoter and enhancer activities are dampened by FLS-359 (Fig. 7D). Consistent with our observation, the full-length, SIRT2 isoform 1 (SIRT2.1) has been shown to facilitate HBV transcription templated from either cccDNA or HBV plasmids following transient transfection, by positively regulating all four HBV promoters (Piracha et al., 2018). SIRT2 has been reported to support HBV transcription by reducing infected-cell p53 levels, thereby alleviating the repressive effect of p53 binding at two viral promoter/-enhancer regions, EnI/Xp and EnII/Cp (Wu et al., 2022). Another recent study suggested that SIRT2 deacetylates and stabilizes the hepatocyte nuclear factor 4α (HNF4α) protein, a liver enriched transcription factor fueling HBV transcription (Ren et al., 2021; Tang and McLachlan, 2001).

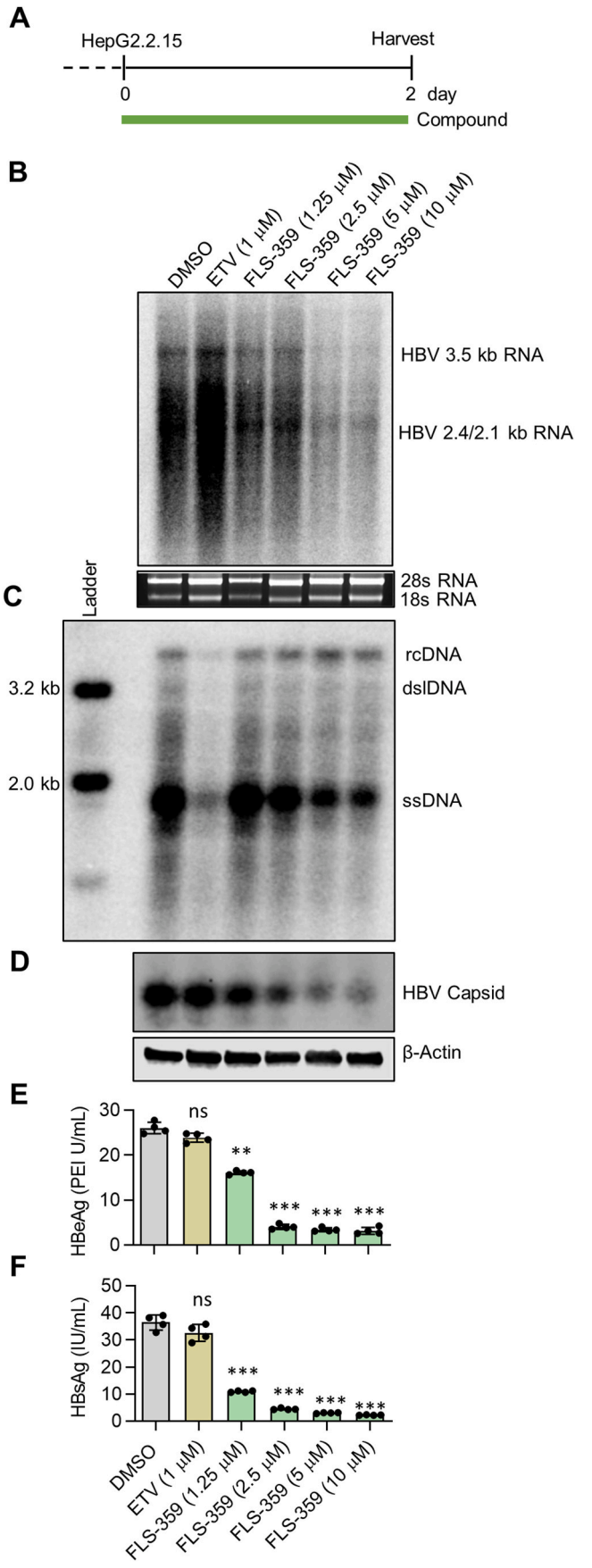

(caption on next column)

Fig. 5. FLS-359 hampers HBV RNA, DNA and protein production in HepG2.2.15 cells. (A) Schematic representation of the compound treatment. HepG2.2.15 cells were treated with DMSO, ETV (1 μM) or FLS-359 at indicated concentrations. Cells and culture supernatant were harvested 2 days after drug treatment. (**B**) Total RNA was extracted from cells and analyzed by Northern blot assay using a ^{32}P-labeled full-length minus strand HBV riboprobe. HBV 3.5 kb RNA and 2.4/2.1 kb RNA species are labeled. 18 S and 28 S ribosomal RNA serve as loading controls. (**C**) Replicative cytoplasmic core DNA was analyzed by Southern blot assay using a ^{32}P-labeled full-length plus strand HBV riboprobe. rcDNA and ssDNA are labeled. (**D**) HBV capsid was detected by using a particle gel assay. β-actin protein levels were determined by Western blot assay using same number of cells as used to quantify capsids. (**E-F**) Secreted HBeAg and HBsAg that accumulated during the 2-day treatment was quantified by CLIA assay. Mean ± SD is shown (n = 4). $^{**}p < 0.01$, $^{***}p < 0.001$.

Whether FLS-359 works through p53, HNF4α or both to antagonize HBV transcription needs to be further investigated.

Integrated HBV DNA has proven to contribute to high serum HBsAg levels and CHB pathogenesis (Wooddell et al., 2017). Therefore, not only cccDNA but also integrated HBV DNA must be eliminated or inactivated by therapeutics to restore a functional anti-HBV immune response (Ghany and Lok, 2022; Tang et al., 2017; Yang et al., 2021). Neither NUCs nor IFN-α directly antagonize integrated HBV gene expression. In contrast, FLS-359 hampers accumulation of HBV RNA, DNA, capsids, and HBsAg in HepG2.2.15 cells (Fig. 5), which serve as a model for the activity of integrated HBV DNA (Sureau et al., 1986). The impact of the drug on HBV promoter activities (Fig. 7) can explain the reduced virologic markers we observed in HepG2.2.15 cells after FLS-359 treatment. Moreover, the fact that FLS-359 curtails the production of HBsAg from integrated HBV DNA more potently than other SIRT2 tool compounds (Fig. S8) emphasizes its promise for therapeutic development.

Extracellular HBsAg or HBeAg were reduced to a greater extent than HBV RNA by FLS-359 (Fig. 6), implying that additional post-transcriptional antiviral mechanisms might be involved. SIRT2 impacts lipid synthesis (Ye et al., 2017), so it is conceivable that FLS-359 alters infected-cell lipid composition, impacting viral processes. Such additional antiviral mechanisms may also explain the marked disproportional changes on ssDNA and rcDNA, when cells were treated with high concentrations of FLS-359 (Fig. 5C).

Chronic HBV infection can cause a weak and exhausted HBV-specific T cell phenotype characterized by poor cytotoxic activity, impaired cytokine production and expression of inhibitory receptors (Fisicaro et al., 2020; Wong et al., 2015). HBsAg accumulates to very high levels, and is thought to drive T-cell exhaustion and deletion (Mueller and Ahmed, 2009). Reducing the amount of HBsAg in the blood could be critical for immune control of chronic HBV infection, and FLS-359 kept HBsAg production at the baseline level in primary hepatocytes (Fig. 3), HepG2.2.15 (Fig. 5 and S8) and C3A-NTCP cells (Fig. 6). Furthermore, SIRT2 inhibition results in enhanced effector function of tumor-reactive T cells through enhanced glycolysis (Hamaidi et al., 2020). It is therefore tempting to speculate that modulation of SIRT2 by FLS-359 could help reactivate exhausted HBV-specific T cells, restoring immune surveillance of the infection.

Although FLS-359 binds and modulates SIRT2 activities in biochemical assays (Roche et al., 2023), it is conceivable that aspects of its anti-HBV activity result from an off-target event. However, multiple chemically distinct SIRT2 tool compounds exhibited similar effects as FLS-359 (Figs. S2, S7, and S8), arguing that SIRT2 modulation constitutes a key element of FLS-359's anti-HBV activity. In addition, compared with knockdown or overexpression of SIRT2 (knockdown or overexpression) that usually resulted in a <2-fold change of HBV replication intermediates (Fig. S3) (Piracha et al., 2018; Wu et al., 2022), treatment with FLS-359 imposed a much more substantial inhibition. The discrepancy could be due to the possibility that FLS-359 inhibits SIRT2 as well as additional cellular pathways required for efficient viral infection. However, as noted above, FLS-359 hampers the

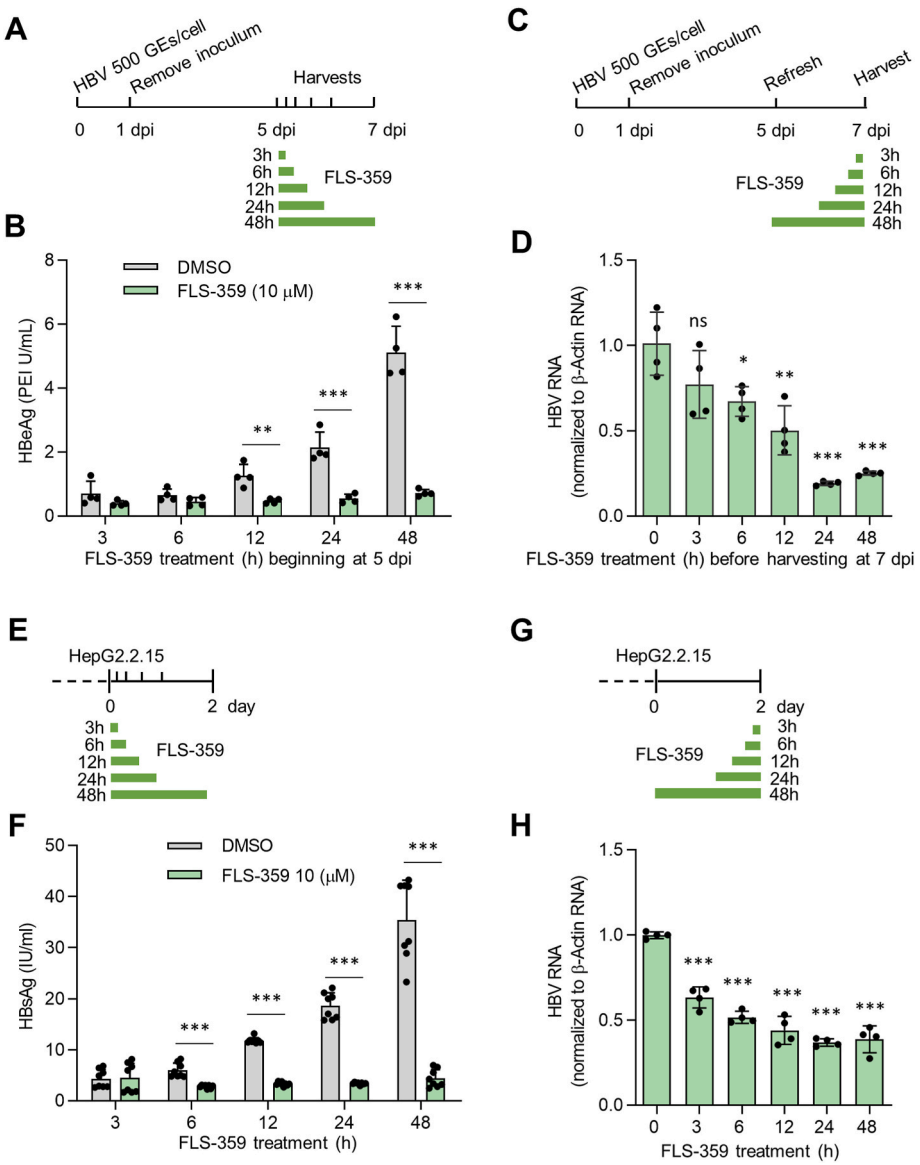

Fig. 6. FLS-359 leads to rapid reduction of viral RNA and antigen in HBV- infected hepatocytes and in HepG2.2.15 cells. (A–B) Schematic representation of the virus infection and compound treatment schedule. C3A-NTCP cells were infected with HBV (500 GE s/cell). At 5 dpi, cells were treated with DMSO or 10 μM FLS-359 in DMSO. Culture supernatants were collected after the indicated time periods of drug treatment, and HBeAg levels were quantified by CLIA assay. (**C-D**) Schematic representation of the virus infection and compound treatment schedule. C3A-NTCP cells were infected with HBV (500 GE s/cell). Cells were harvested at 7 dpi following the indicated periods of treatment with 10 μM FLS-359, and total cell RNA was prepared. Total HBV RNA levels were quantified by qRT-PCR, normalized to β-actin RNA, and results are presented as fold-change relative to the untreated group. (**E-F**) Schematic representation of the compound treatment schedule. HepG2.2.15 cells were treated with DMSO or 10 μM FLS-359 in DMSO. Culture supernatants were collected after indicated periods of drug treatment, and HBsAg levels were quantified by CLIA assay. (**G-H**) Schematic representation of the compound treatment schedule. HepG2.2.15 cells were harvested after the indicated periods of treatment with 10 μM FLS-359 treatment, and total cell RNA was prepared. Total HBV RNA levels were quantified by qRT-PCR, normalized to β-actin RNA, and results are presented as fold-change relative to the untreated group. For all panels, mean ± SD is shown (n = 4). *$p < 0.05$, **$p < 0.01$, ***$p < 0.001$.

de-acetylation activity of SIRT2, but not its de-myristylation activity (Roche et al., 2023). Hence, the drug modulates some but not all SIRT2 activities, so it is not surprising that selective modulation of SIRT2 functions by FLS-359 is not faithfully recapitulated by genetic knock-down or overexpression studies.

In sum, our work demonstrates a multi-faceted mechanism – a block to cccDNA synthesis, reduced viral promoter activity, and likely post-translational effects – by which a small molecule SIRT2 modulator, FLS-359, restricts HBV infection. Considering that SIRT2 knockout mice are healthy (Ciarlo et al., 2017), FLS-359 represents a class of SIRT2 modulators with strong potential for antiviral drug development to treat CHB infection.

CRediT authorship contribution statement

Liudi Tang: Writing – review & editing, Writing – original draft, Methodology, Investigation, Formal analysis, Data curation, Conceptualization. **Stacy Remiszewski:** Writing – review & editing, Project administration, Conceptualization. **Andrew Snedeker:** Methodology, Investigation, Data curation. **Lillian W. Chiang:** Writing – review & editing, Funding acquisition, Conceptualization. **Thomas Shenk:** Writing – review & editing, Supervision, Formal analysis, Conceptualization.

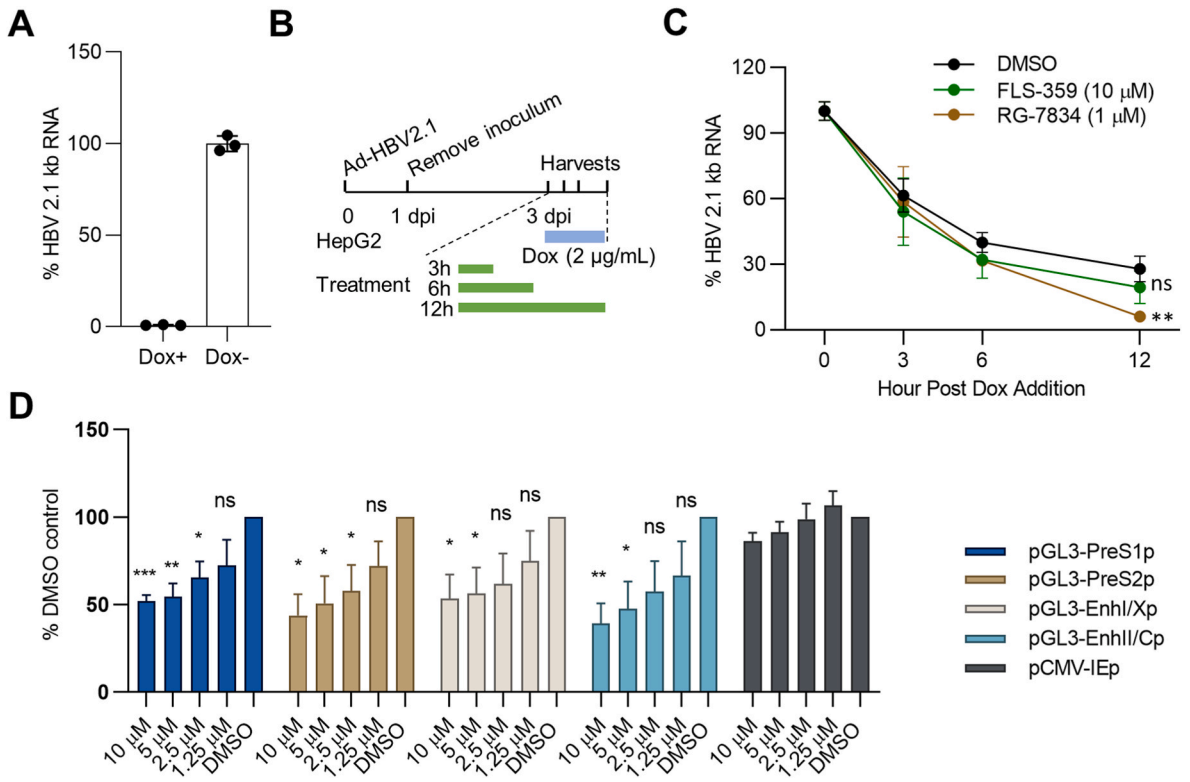

Fig. 7. FLS-359 suppresses HBV RNA production. (A) HepG2 cells infected with Ad-HBV2.1 and cultured in the presence or absence of Dox were harvested at 3 dpi and total cellular RNA was extracted. HBV 2.1 kb RNA was quantified by qRT-PCR, normalized to β-actin RNA, and results are presented as fold-change relative to the Dox-group. Mean ± SD is shown (n = 3). (**B**) Schematic representation of the virus infection and compound treatment schedule. HepG2 cells were infected with Ad-HBV2.1, and cultured in the absence of doxycycline (Dox) for 3 days before shutting down the viral RNA production by switching to medium with Dox (2 μg/ml). Cells were harvested at various times after treatment with DMSO, FLS-359 (10 μM in DMSO) or RG-7834 (10 μM in DMSO). (**C**) HBV 2.1 kb RNA was measured by qRT-PCR, normalized to β-actin RNA. Mean ± SD is shown (n = 3). (**D**) HepG2 cells were transfected with reporters containing each of the four HBV promoters or a control HCMV promoter (IEp) for 24 h and then treated with FLS-359 at indicated concentrations for another 24 h before performing luciferase assays. The absolute luciferase levels for drug-treated cells are presented as a percentage of the level for cells treated with DMSO. Mean ± SD is shown (n = 3). *$p < 0.05$, **$p < 0.01$, ***$p < 0.001$.

Declaration of competing interest

The authors declare the following financial interests/personal relationships which may be considered as potential competing interests.

Data availability

Data will be made available on request.

Acknowledgements

We thank Ju-Tao Guo (Baruch S. Blumberg Institute) for providing C3A-NTCP cells and HBV genotypes A, B, C, and D plasmids; Christoph Seeger (Fox Chase Cancer Center) for providing HepAD38 cells; Tianlun Zhou (Baruch S. Blumberg Institute) for providing Ad-HBV2.1; Eain Murphy (Upstate Medical University) for providing pGL3-CMV-IEp plasmid. We thank Ju-Tao Guo and Timothy Block for insightful discussions. This work received support from NIH (R44-AI157725).

Appendix A. Supplementary data

Supplementary data to this article can be found online at https://doi.org/10.1016/j.antiviral.2024.105888.

References

Allweiss, L., Giersch, K., Pirosu, A., Volz, T., Muench, R.C., Beran, R.K., Urban, S., Javanbakht, H., Fletcher, S.P., Lutgehetmann, M., Dandri, M., 2022. Therapeutic shutdown of HBV transcripts promotes reappearance of the SMC5/6 complex and silencing of the viral genome in vivo. Gut 71, 372–381. https://doi.org/10.1136/gutjnl-2020-322571.

Alter, H., Block, T., Brown, N., Brownstein, A., Brosgart, C., Chang, K.M., Chen, P.J., Chisari, F.V., Cohen, C., El-Serag, H., Feld, J., Gish, R., Glenn, J., Greten, T., Guo, H., Guo, J.T., Hoshida, Y., Hu, J., Kowdley, K.V., Li, W., Liang, J., Locarnini, S., Lok, A. S., Mason, W., McMahon, B., Mehta, A., Perrillo, R., Revill, P., Rice, C.M., Rinaudo, J., Schinazi, R., Seeger, C., Shetty, K., Tavis, J., Zoulim, F., 2018. A research agenda for curing chronic hepatitis B virus infection. Hepatology 67, 1127–1131. https://doi.org/10.1002/hep.29509.

Bill, C.A., Summers, J., 2004. Genomic DNA double-strand breaks are targets for hepadnaviral DNA integration. Proc. Natl. Acad. Sci. U. S. A. 101, 11135–11140. https://doi.org/10.1073/pnas.0403925101.

Bloom, K., Maepa, M.B., Ely, A., Arbuthnot, P., 2018. Gene therapy for chronic HBV-can we eliminate cccDNA? Genes (Basel) 9. https://doi.org/10.3390/genes9040207.

Boyd, A., Lacombe, K., Lavocat, F., Maylin, S., Miailhes, P., Lascoux-Combe, C., Delaugerre, C., Girard, P.M., Zoulim, F., 2016. Decay of ccc-DNA marks persistence of intrahepatic viral DNA synthesis under tenofovir in HIV-HBV co-infected patients. J. Hepatol. 65, 683–691. https://doi.org/10.1016/j.jhep.2016.05.014.

Chakraborty, A., Ko, C., Henning, C., Lucko, A., Harris, J.M., Chen, F., Zhuang, X., Wettengel, J.M., Roessler, S., Protzer, U., McKeating, J.A., 2020. Synchronised infection identifies early rate-limiting steps in the hepatitis B virus life cycle. Cell Microbiol. 22, e13250 https://doi.org/10.1111/cmi.13250.

Chen, Y.C., Koutelou, E., Dent, S.Y.R., 2022. Now open: evolving insights to the roles of lysine acetylation in chromatin organization and function. Mol. Cell 82, 716–727. https://doi.org/10.1016/j.molcel.2021.12.004.

Cheng, J., Zhao, Q., Zhou, Y., Tang, L., Sheraz, M., Chang, J., Guo, J.T., 2020. Interferon alpha induces multiple cellular proteins that coordinately suppress hepadnaviral covalently closed circular DNA transcription. J. Virol. 94 https://doi.org/10.1128/JVI.00442-20.

Cheng, S.T., Ren, J.H., Cai, X.F., Jiang, H., Chen, J., 2018. HBx-elevated SIRT2 promotes HBV replication and hepatocarcinogenesis. Biochem. Biophys. Res. Commun. 496, 904–910. https://doi.org/10.1016/j.bbrc.2018.01.127.

Ciarlo, E., Heinonen, T., Theroude, C., Herderschee, J., Mombelli, M., Lugrin, J., Pfefferle, M., Tyrrell, B., Lensch, S., Acha-Orbea, H., Le Roy, D., Auwerx, J., Roger, T., 2017. Sirtuin 2 deficiency increases bacterial phagocytosis by

Macrophages and protects from chronic staphylococcal infection. Front. Immunol. 8, 1037. https://doi.org/10.3389/fimmu.2017.01037.
Feldman, J.L., Baeza, J., Denu, J.M., 2013. Activation of the protein deacetylase SIRT6 by long-chain fatty acids and widespread deacylation by mammalian sirtuins. J. Biol. Chem. 288, 31350–31356. https://doi.org/10.1074/jbc.C113.511261.
Feldman, J.L., Dittenhafer-Reed, K.E., Denu, J.M., 2012. Sirtuin catalysis and regulation. J. Biol. Chem. 287, 42419–42427. https://doi.org/10.1074/jbc.R112.378877.
Fisicaro, P., Barili, V., Rossi, M., Montali, I., Vecchi, A., Acerbi, G., Laccabue, D., Zecca, A., Penna, A., Missale, G., Ferrari, C., Boni, C., 2020. Pathogenetic mechanisms of T cell dysfunction in chronic HBV infection and related therapeutic approaches. Front. Immunol. 11, 849. https://doi.org/10.3389/fimmu.2020.00849.
Ghany, M.G., Lok, A.S., 2022. Functional cure of hepatitis B requires silencing covalently closed circular and integrated hepatitis B virus DNA. J. Clin. Invest. 132 https://doi.org/10.1172/JCI163175.
Guo, F., Zhao, Q., Sheraz, M., Cheng, J., Qi, Y., Su, Q., Cuconati, A., Wei, L., Du, Y., Li, W., Chang, J., Guo, J.T., 2017. HBV core protein allosteric modulators differentially alter cccDNA biosynthesis from de novo infection and intracellular amplification pathways. PLoS Pathog. 13, e1006658 https://doi.org/10.1371/journal.ppat.1006658.
Guo, J.T., Guo, H., 2015. Metabolism and function of hepatitis B virus cccDNA: implications for the development of cccDNA-targeting antiviral therapeutics. Antivir. Res. 122, 91–100. https://doi.org/10.1016/j.antiviral.2015.08.005.
Hackett, B.A., Dittmar, M., Segrist, E., Pittenger, N., To, J., Griesman, T., Gordesky-Gold, B., Schultz, D.C., Cherry, S., 2019. Sirtuin inhibitors are broadly antiviral against arboviruses. mBio 10. https://doi.org/10.1128/mBio.01446-19.
Hamaidi, I., Zhang, L., Kim, N., Wang, M.H., Iclozan, C., Fang, B., Liu, M., Koomen, J.M., Berglund, A.E., Yoder, S.J., Yao, J., Engelman, R.W., Creelan, B.C., Conejo-Garcia, J. R., Antonia, S.J., Mule, J.J., Kim, S., 2020. Sirt2 inhibition enhances metabolic fitness and effector functions of tumor-reactive T cells. Cell Metabol. 32, 420–436 e412. https://doi.org/10.1016/j.cmet.2020.07.008.
Han, X., Zhou, C., Jiang, M., Wang, Y., Wang, J., Cheng, Z., Wang, M., Liu, Y., Liang, C., Wang, J., Wang, Z., Weikert, R., Lv, W., Xie, J., Yu, X., Zhou, X., Luangsay, S., Shen, H.C., Mayweg, A.V., Javanbakht, H., Yang, S., 2018. Discovery of RG7834: the first-in-class selective and orally available small molecule hepatitis B virus expression inhibitor with novel mechanism of action. J. Med. Chem. 61, 10619–10634. https://doi.org/10.1021/acs.jmedchem.8b01245.
Heltweg, B., Gatbonton, T., Schuler, A.D., Posakony, J., Li, H., Goehle, S., Kollipara, R., Depinho, R.A., Gu, Y., Simon, J.A., Bedalov, A., 2006. Antitumor activity of a small-molecule inhibitor of human silent information regulator 2 enzymes. Cancer Res. 66, 4368–4377. https://doi.org/10.1158/0008-5472.CAN-05-3617.
Hoff, K.G., Avalos, J.L., Sens, K., Wolberger, C., 2006. Insights into the sirtuin mechanism from ternary complexes containing NAD+ and acetylated peptide. Structure 14, 1231–1240. https://doi.org/10.1016/j.str.2006.06.006.
Hsu, Y.C., Huang, D.Q., Nguyen, M.H., 2023. Global burden of hepatitis B virus: current status, missed opportunities and a call for action. Nat. Rev. Gastroenterol. Hepatol. 20, 524–537. https://doi.org/10.1038/s41575-023-00760-9.
Hu, J., Liu, K., 2017. Complete and incomplete hepatitis B virus particles: formation, function, and application. Viruses 9. https://doi.org/10.3390/v9030056.
Huang, H.C., Chen, C.C., Chang, W.C., Tao, M.H., Huang, C., 2012. Entry of hepatitis B virus into immortalized human primary hepatocytes by clathrin-dependent endocytosis. J. Virol. 86, 9443–9453. https://doi.org/10.1128/JVI.00873-12.
Huang, Q., Zhou, B., Cai, D., Zong, Y., Wu, Y., Liu, S., Mercier, A., Guo, H., Hou, J., Colonno, R., Sun, J., 2021. Rapid turnover of hepatitis B virus covalently closed circular DNA indicated by monitoring emergence and reversion of signature-mutation in treated chronic hepatitis B patients. Hepatology 73, 41–52. https://doi.org/10.1002/hep.31240.
Jeng, W.J., Lok, A.S., 2021. Should treatment indications for chronic hepatitis B Be expanded? Clin. Gastroenterol. Hepatol. 19, 2006–2014. https://doi.org/10.1016/j.cgh.2020.04.091.
Jiang, H., Cheng, S.T., Ren, J.H., Ren, F., Yu, H.B., Wang, Q., Huang, A.L., Chen, J., 2019. SIRT6 inhibitor, OSS_128167 restricts hepatitis B virus transcription and replication through targeting transcription factor peroxisome proliferator-activated receptors alpha. Front. Pharmacol. 10, 1270. https://doi.org/10.3389/fphar.2019.01270.
Jin, Y., Wang, S., Xu, S., Zhao, S., Xu, X., Poongavanam, V., Menendez-Arias, L., Zhan, P., Liu, X., 2023. Targeting hepatitis B virus cccDNA levels: recent progress in seeking small molecule drug candidates. Drug Discov. Today 28, 103617. https://doi.org/10.1016/j.drudis.2023.103617.
Jing, H., Hu, J., He, B., Negron Abril, Y.L., Stupinski, J., Weiser, K., Carbonaro, M., Chiang, Y.L., Southard, T., Giannakakou, P., Weiss, R.S., Lin, H., 2016. A SIRT2-selective inhibitor promotes c-Myc oncoprotein degradation and exhibits broad anticancer activity. Cancer Cell 29, 767–768. https://doi.org/10.1016/j.ccell.2016.04.005.
Koyuncu, E., Budayeva, H.G., Miteva, Y.V., Ricci, D.P., Silhavy, T.J., Shenk, T., Cristea, I. M., 2014. Sirtuins are evolutionarily conserved viral restriction factors. mBio 5. https://doi.org/10.1128/mBio.02249-14.
Ladner, S.K., Otto, M.J., Barker, C.S., Zaifert, K., Wang, G.H., Guo, J.T., Seeger, C., King, R.W., 1997. Inducible expression of human hepatitis B virus (HBV) in stably transfected hepatoblastoma cells: a novel system for screening potential inhibitors of HBV replication. Antimicrob. Agents Chemother. 41, 1715–1720. https://doi.org/10.1128/AAC.41.8.1715.
Lai, C.L., Wong, D., Ip, P., Kopaniszen, M., Seto, W.K., Fung, J., Huang, F.Y., Lee, B., Cullaro, G., Chong, C.K., Wu, R., Cheng, C., Yuen, J., Ngai, V., Yuen, M.F., 2017. Reduction of covalently closed circular DNA with long-term nucleos(t)ide analogue treatment in chronic hepatitis B. J. Hepatol. 66, 275–281. https://doi.org/10.1016/j.jhep.2016.08.022.
Lee, S., Goyal, A., Perelson, A.S., Ishida, Y., Saito, T., Gale Jr., M., 2021. Suppression of hepatitis B virus through therapeutic activation of RIG-I and IRF3 signaling in hepatocytes. iScience 24, 101969. https://doi.org/10.1016/j.isci.2020.101969.
Liang, T.J., Block, T.M., McMahon, B.J., Ghany, M.G., Urban, S., Guo, J.T., Locarnini, S., Zoulim, F., Chang, K.M., Lok, A.S., 2015. Present and future therapies of hepatitis B: from discovery to cure. Hepatology 62, 1893–1908. https://doi.org/10.1002/hep.28025.
Lin, H., 2023. Substrate-selective small-molecule modulators of enzymes: mechanisms and opportunities. Curr. Opin. Chem. Biol. 72, 102231 https://doi.org/10.1016/j.cbpa.2022.102231.
Lucifora, J., Xia, Y., Reisinger, F., Zhang, K., Stadler, D., Cheng, X., Sprinzl, M.F., Koppensteiner, H., Makowska, Z., Volz, T., Remouchamps, C., Chou, W.M., Thasler, W.E., Huser, N., Durantel, D., Liang, T.J., Munk, C., Heim, M.H., Browning, J.L., Dejardin, E., Dandri, M., Schindler, M., Heikenwalder, M., Protzer, U., 2014. Specific and nonhepatotoxic degradation of nuclear hepatitis B virus cccDNA. Science 343, 1221–1228. https://doi.org/10.1126/science.1243462.
Macovei, A., Radulescu, C., Lazar, C., Petrescu, S., Durantel, D., Dwek, R.A., Zitzmann, N., Nichita, N.B., 2010. Hepatitis B virus requires intact caveolin-1 function for productive infection in HepaRG cells. J. Virol. 84, 243–253. https://doi.org/10.1128/JVI.01207-09.
Martinez, M.G., Boyd, A., Combe, E., Testoni, B., Zoulim, F., 2021. Covalently closed circular DNA: the ultimate therapeutic target for curing HBV infections. J. Hepatol. 75, 706–717. https://doi.org/10.1016/j.jhep.2021.05.013.
Mueller, H., Lopez, A., Tropberger, P., Wildum, S., Schmaler, J., Pedersen, L., Han, X., Wang, Y., Ottosen, S., Yang, S., Young, J.A.T., Javanbakht, H., 2019. PAPD5/7 are host factors that are required for hepatitis B virus RNA stabilization. Hepatology 69, 1398–1411. https://doi.org/10.1002/hep.30329.
Mueller, H., Wildum, S., Luangsay, S., Walther, J., Lopez, A., Tropberger, P., Ottaviani, G., Lu, W., Parrott, N.J., Zhang, J.D., Schmucki, R., Racek, T., Hoflack, J. C., Kueng, E., Point, F., Zhou, X., Steiner, G., Lutgehetmann, M., Rapp, G., Volz, T., Dandri, M., Yang, S., Young, J.A.T., Javanbakht, H., 2018. A novel orally available small molecule that inhibits hepatitis B virus expression. J. Hepatol. 68, 412–420. https://doi.org/10.1016/j.jhep.2017.10.014.
Mueller, S.N., Ahmed, R., 2009. High antigen levels are the cause of T cell exhaustion during chronic viral infection. Proc. Natl. Acad. Sci. U. S. A. 106, 8623–8628. https://doi.org/10.1073/pnas.0809818106.
Nassal, M., 2015. HBV cccDNA: viral persistence reservoir and key obstacle for a cure of chronic hepatitis B. Gut 64, 1972–1984. https://doi.org/10.1136/gutjnl-2015-309809.
Okada, A.K., Teranishi, K., Ambroso, M.R., Isas, J.M., Vazquez-Sarandeses, E., Lee, J.Y., Melo, A.A., Pandey, P., Merken, D., Berndt, L., Lammers, M., Daumke, O., Chang, K., Haworth, I.S., Langen, R., 2021. Lysine acetylation regulates the interaction between proteins and membranes. Nat. Commun. 12, 6466. https://doi.org/10.1038/s41467-021-26657-2.
Peng, B., Jing, Z., Zhou, Z., Sun, Y., Guo, G., Tan, Z., Diao, Y., Yao, Q., Ping, Y., Li, X., Ren, T., Li, B., Li, W., 2023. Nonproductive hepatitis B virus covalently closed circular DNA generates HBx-related transcripts from the HBx/enhancer I region and acquires reactivation by superinfection in single cells. J. Virol. 97, e0171722 https://doi.org/10.1128/jvi.01717-22.
Piracha, Z.Z., Kwon, H., Saeed, U., Kim, J., Jung, J., Chwae, Y.J., Park, S., Shin, H.J., Kim, K., 2018. Sirtuin 2 isoform 1 enhances hepatitis B virus RNA transcription and DNA synthesis through the AKT/GSK-3beta/beta-Catenin signaling pathway. J. Virol. 92 https://doi.org/10.1128/JVI.00955-18.
Piracha, Z.Z., Saeed, U., Kim, J., Kwon, H., Chwae, Y.J., Lee, H.W., Lim, J.H., Park, S., Shin, H.J., Kim, K., 2020. An alternatively spliced sirtuin 2 isoform 5 inhibits hepatitis B virus replication from cccDNA by repressing epigenetic modifications made by histone lysine methyltransferases. J. Virol. 94 https://doi.org/10.1128/JVI.00926-20.
Poniewierska-Baran, A., Warias, P., Zgutka, K., 2022. Sirtuins (SIRTs) as a novel target in gastric cancer. Int. J. Mol. Sci. 23 https://doi.org/10.3390/ijms232315119.
Qi, Y., Gao, Z., Xu, G., Peng, B., Liu, C., Yan, H., Yao, Q., Sun, G., Liu, Y., Tang, D., Song, Z., He, W., Sun, Y., Guo, J.T., Li, W., 2016. DNA polymerase kappa is a key cellular factor for the formation of covalently closed circular DNA of hepatitis B virus. PLoS Pathog. 12, e1005893 https://doi.org/10.1371/journal.ppat.1005893.
Qu, B., Nebioglu, F., Leuthold, M.M., Ni, Y., Mutz, P., Beneke, J., Erfle, H., Vondran, F.W. R., Bartenschlager, R., Urban, S., 2022. Dual role of neddylation in transcription of hepatitis B virus RNAs from cccDNA and production of viral surface antigen. JHEP Rep 4, 100551. https://doi.org/10.1016/j.jhepr.2022.100551.
Ren, H., Hu, F., Wang, D., Kang, X., Feng, X., Zhang, L., Zhou, B., Liu, S., Yuan, G., 2021. Sirtuin 2 prevents liver steatosis and metabolic disorders by deacetylation of hepatocyte nuclear factor 4alpha. Hepatology 74, 723–740. https://doi.org/10.1002/hep.31773.
Ren, J.H., Hu, J.L., Cheng, S.T., Yu, H.B., Wong, V.K.W., Law, B.Y.K., Yang, Y.F., Huang, Y., Liu, Y., Chen, W.X., Cai, X.F., Tang, H., Hu, Y., Zhang, W.L., Liu, X., Long, Q.X., Zhou, L., Tao, N.N., Zhou, H.Z., Yang, Q.X., Ren, F., He, L., Gong, R., Huang, A.L., Chen, J., 2018. SIRT3 restricts hepatitis B virus transcription and replication through epigenetic regulation of covalently closed circular DNA involving suppressor of variegation 3-9 homolog 1 and SET domain containing 1A histone methyltransferases. Hepatology 68, 1260–1276. https://doi.org/10.1002/hep.29912.
Ren, J.H., Tao, Y., Zhang, Z.Z., Chen, W.X., Cai, X.F., Chen, K., Ko, B.C., Song, C.L., Ran, L.K., Li, W.Y., Huang, A.L., Chen, J., 2014. Sirtuin 1 regulates hepatitis B virus transcription and replication by targeting transcription factor AP-1. J. Virol. 88, 2442–2451. https://doi.org/10.1128/JVI.02861-13.
Roche, K.L., Remiszewski, S., Todd, M.J., Kulp 3rd, J.L., Tang, L., Welsh, A.V., Barry, A. P., De, C., Reiley, W.W., Wahl, A., Garcia, J.V., Luftig, M.A., Shenk, T., Tonra, J.R.,

Murphy, E.A., Chiang, L.W., 2023. An allosteric inhibitor of sirtuin 2 deacetylase activity exhibits broad-spectrum antiviral activity. J. Clin. Invest. 133 https://doi.org/10.1172/JCI158978.

Rumpf, T., Schiedel, M., Karaman, B., Roessler, C., North, B.J., Lehotzky, A., Olah, J., Ladwein, K.I., Schmidtkunz, K., Gajer, M., Pannek, M., Steegborn, C., Sinclair, D.A., Gerhardt, S., Ovadi, J., Schutkowski, M., Sippl, W., Einsle, O., Jung, M., 2015. Selective Sirt2 inhibition by ligand-induced rearrangement of the active site. Nat. Commun. 6, 6263. https://doi.org/10.1038/ncomms7263.

Shen, F., Li, Y., Wang, Y., Sozzi, V., Revill, P.A., Liu, J., Gao, L., Yang, G., Lu, M., Sutter, K., Dittmer, U., Chen, J., Yuan, Z., 2018. Hepatitis B virus sensitivity to interferon-alpha in hepatocytes is more associated with cellular interferon response than with viral genotype. Hepatology 67, 1237–1252. https://doi.org/10.1002/hep.29609.

Sheraz, M., Cheng, J., Tang, L., Chang, J., Guo, J.T., 2019. Cellular DNA topoisomerases are required for the synthesis of hepatitis B virus covalently closed circular DNA. J. Virol. 93 https://doi.org/10.1128/JVI.02230-18.

Stadler, D., Kachele, M., Jones, A.N., Hess, J., Urban, C., Schneider, J., Xia, Y., Oswald, A., Nebioglu, F., Bester, R., Lasitschka, F., Ringelhan, M., Ko, C., Chou, W. M., Geerlof, A., van de Klundert, M.A., Wettengel, J.M., Schirmacher, P., Heikenwalder, M., Schreiner, S., Bartenschlager, R., Pichlmair, A., Sattler, M., Unger, K., Protzer, U., 2021. Interferon-induced degradation of the persistent hepatitis B virus cccDNA form depends on ISG20. EMBO Rep. 22, e49568 https://doi.org/10.15252/embr.201949568.

Sun, L., Zhang, F., Guo, F., Liu, F., Kulsuptrakul, J., Puschnik, A., Gao, M., Rijnbrand, R., Sofia, M., Block, T., Zhou, T., 2020. The dihydroquinolizinone compound RG7834 inhibits the polyadenylase function of PAPD5 and PAPD7 and accelerates the degradation of matured hepatitis B virus surface protein mRNA. Antimicrob. Agents Chemother. 65 https://doi.org/10.1128/AAC.00640-20.

Sureau, C., Romet-Lemonne, J.L., Mullins, J.I., Essex, M., 1986. Production of hepatitis B virus by a differentiated human hepatoma cell line after transfection with cloned circular HBV DNA. Cell 47, 37–47. https://doi.org/10.1016/0092-8674(86)90364-8.

Tang, H., McLachlan, A., 2001. Transcriptional regulation of hepatitis B virus by nuclear hormone receptors is a critical determinant of viral tropism. Proc. Natl. Acad. Sci. U. S. A. 98, 1841–1846. https://doi.org/10.1073/pnas.98.4.1841.

Tang, L., Sheraz, M., McGrane, M., Chang, J., Guo, J.T., 2019. DNA Polymerase alpha is essential for intracellular amplification of hepatitis B virus covalently closed circular DNA. PLoS Pathog. 15, e1007742 https://doi.org/10.1371/journal.ppat.1007742.

Tang, L., Zhao, Q., Wu, S., Cheng, J., Chang, J., Guo, J.T., 2017. The current status and future directions of hepatitis B antiviral drug discovery. Expet Opin. Drug Discov. 12, 5–15. https://doi.org/10.1080/17460441.2017.1255195.

Teixeira, C.S.S., Cerqueira, N., Gomes, P., Sousa, S.F., 2020. A molecular perspective on sirtuin activity. Int. J. Mol. Sci. 21 https://doi.org/10.3390/ijms21228609.

Testoni, B., Ploss, A., 2023. Cracking the host functional network involved in hepatitis B virus cccDNA biology. Gut 72, 1637–1639. https://doi.org/10.1136/gutjnl-2022-329185.

Tropberger, P., Mercier, A., Robinson, M., Zhong, W., Ganem, D.E., Holdorf, M., 2015. Mapping of histone modifications in episomal HBV cccDNA uncovers an unusual chromatin organization amenable to epigenetic manipulation. Proc. Natl. Acad. Sci. U. S. A. 112, E5715–E5724. https://doi.org/10.1073/pnas.1518090112.

Tu, T., Budzinska, M.A., Shackel, N.A., Urban, S., 2017. HBV DNA integration: molecular mechanisms and clinical implications. Viruses 9. https://doi.org/10.3390/v9040075.

Tuttleman, J.S., Pourcel, C., Summers, J., 1986. Formation of the pool of covalently closed circular viral DNA in hepadnavirus-infected cells. Cell 47, 451–460. https://doi.org/10.1016/0092-8674(86)90602-1.

Wang, L., Zhu, Q., Zhang, J.D., Zhang, Y., Ni, X., Xiang, K., Jiang, J., Li, B., Yu, Y., Hu, H., Zhang, M., Wu, W., Zeng, J., Yan, Z., Dai, J., Sun, K., Zhang, X., Chen, D., Feng, S., Sach-Peltason, L., Young, J.A.T., Gao, L., 2023. Discovery of a first-in-class orally available HBV cccDNA inhibitor. J. Hepatol. 78, 742–753. https://doi.org/10.1016/j.jhep.2022.12.014.

Wang, T., Xu, Z., Lu, Y., Shi, J., Liu, W., Zhang, C., Jiang, Z., Qi, B., Bai, L., 2019. Recent progress on the discovery of Sirt2 inhibitors for the treatment of various cancers. Curr. Top. Med. Chem. 19, 1051–1058. https://doi.org/10.2174/1568026619666190510103416.

Wei, L., Ploss, A., 2021. Mechanism of hepatitis B virus cccDNA formation. Viruses 13. https://doi.org/10.3390/v13081463.

Wong, Y.C., Tay, S.S., McCaughan, G.W., Bowen, D.G., Bertolino, P., 2015. Immune outcomes in the liver: is CD8 T cell fate determined by the environment? J. Hepatol. 63, 1005–1014. https://doi.org/10.1016/j.jhep.2015.05.033.

Wooddell, C.I., Yuen, M.F., Chan, H.L., Gish, R.G., Locarnini, S.A., Chavez, D., Ferrari, C., Given, B.D., Hamilton, J., Kanner, S.B., Lai, C.L., Lau, J.Y.N., Schluep, T., Xu, Z., Lanford, R.E., Lewis, D.L., 2017. RNAi-based treatment of chronically infected patients and chimpanzees reveals that integrated hepatitis B virus DNA is a source of HBsAg. Sci. Transl. Med. 9 https://doi.org/10.1126/scitranslmed.aan0241.

Wu, D.Q., Ding, Q.Y., Tao, N.N., Tan, M., Zhang, Y., Li, F., Zhou, Y.J., Dong, M.L., Cheng, S.T., Ren, F., Chen, J., Ren, J.H., 2022. SIRT2 promotes HBV transcription and replication by targeting transcription factor p53 to increase the activities of HBV enhancers and promoters. Front. Microbiol. 13, 836446 https://doi.org/10.3389/fmicb.2022.836446.

Wu, S., Luo, Y., Viswanathan, U., Kulp, J., Cheng, J., Hu, Z., Xu, Q., Zhou, Y., Gong, G.Z., Chang, J., Li, Y., Guo, J.T., 2018. CpAMs induce assembly of HBV capsids with altered electrophoresis mobility: implications for mechanism of inhibiting pgRNA packaging. Antivir. Res. 159, 1–12. https://doi.org/10.1016/j.antiviral.2018.09.001.

Xia, Y., Guo, H., 2020. Hepatitis B virus cccDNA: formation, regulation and therapeutic potential. Antivir. Res. 180, 104824 https://doi.org/10.1016/j.antiviral.2020.104824.

Xia, Y., Stadler, D., Ko, C., Protzer, U., 2017. Analyses of HBV cccDNA quantification and modification. Methods Mol. Biol. 1540, 59–72. https://doi.org/10.1007/978-1-4939-6700-1_6.

Xia, Y., Stadler, D., Lucifora, J., Reisinger, F., Webb, D., Hosel, M., Michler, T., Wisskirchen, K., Cheng, X., Zhang, K., Chou, W.M., Wettengel, J.M., Malo, A., Bohne, F., Hoffmann, D., Eyer, F., Thimme, R., Falk, C.S., Thasler, W.E., Heikenwalder, M., Protzer, U., 2016. Interferon-gamma and tumor necrosis factor-alpha produced by T cells reduce the HBV persistence form, cccDNA, without cytolysis. Gastroenterology 150, 194–205. https://doi.org/10.1053/j.gastro.2015.09.026.

Yang, S., Zeng, W., Zhang, J., Lu, F., Chang, J., Guo, J.T., 2021. Restoration of a functional antiviral immune response to chronic HBV infection by reducing viral antigen load: if not sufficient, is it necessary? Emerg. Microb. Infect. 10, 1545–1554. https://doi.org/10.1080/22221751.2021.1952851.

Ye, X., Li, M., Hou, T., Gao, T., Zhu, W.G., Yang, Y., 2017. Sirtuins in glucose and lipid metabolism. Oncotarget 8, 1845–1859. https://doi.org/10.18632/oncotarget.12157.

Yu, H.B., Cheng, S.T., Ren, F., Chen, Y., Shi, X.F., Wong, V.K.W., Law, B.Y.K., Ren, J.H., Zhong, S., Chen, W.X., Xu, H.M., Zhang, Z.Z., Hu, J.L., Cai, X.F., Hu, Y., Zhang, W.L., Long, Q.X., He, L., Hu, Z.W., Jiang, H., Zhou, H.Z., Huang, A.L., Chen, J., 2021. SIRT7 restricts HBV transcription and replication through catalyzing desuccinylation of histone H3 associated with cccDNA minichromosome. Clin. Sci. (Lond.) 135, 1505–1522. https://doi.org/10.1042/CS20210392.

Yu, H.B., Jiang, H., Cheng, S.T., Hu, Z.W., Ren, J.H., Chen, J., 2018. AGK2, A SIRT2 inhibitor, inhibits hepatitis B virus replication in vitro and in vivo. Int. J. Med. Sci. 15, 1356–1364. https://doi.org/10.7150/ijms.26125.

Zoulim, F., Testoni, B., 2023. Eliminating cccDNA to cure hepatitis B virus infection. J. Hepatol. 78, 677–680. https://doi.org/10.1016/j.jhep.2023.01.017.